Am J Cancer Res 2023;13(12):6241-6255
www.ajcr.us /ISSN:2156-6976/ajcr0150143

Original Article

Novel combination of imipridones and histone deacetylase inhibitors demonstrate cytotoxic effect through integrated stress response in pediatric solid tumors

Wen-I Chang[1,2,4,5], Joshua N Honeyman[1,3,4,5], Jun Zhang[1,4,5,6], Claire Lin[1,4,5,6], Aditi Sharma[1,6], Lanlan Zhou[1,4,5,6], Janice Oliveira[1,6], Nikos Tapinos[4,5,7], Rishi R Lulla[2,4,5], Varun V Prabhu[8], Wafik S El-Deiry[1,4,5,6,9]

[1]Laboratory of Translational Oncology and Translational Cancer Therapeutics, Warren Alpert Medical School of Brown University, Providence, RI, USA; [2]Division of Pediatric Hematology/Oncology, Department of Pediatrics, Brown University, Providence, RI, USA; [3]Division of Pediatric Surgery, Department of Surgery, Brown University, Providence, RI, USA; [4]Legorreta Cancer Center, Brown University, Providence, RI, USA; [5]Joint Program in Cancer Biology, Brown University and Lifespan Cancer Institute, Providence, RI, USA; [6]Department of Pathology and Laboratory Medicine, Brown University, Providence, RI, USA; [7]Department of Neurosurgery, Warren Alpert Medical School of Brown University, Providence, RI, USA; [8]Chimerix Inc., Durham, NC, USA; [9]Division of Hematology/Oncology, Department of Medicine, Lifespan and Brown University, Providence, RI, USA

Received March 14, 2023; Accepted November 14, 2023; Epub December 15, 2023; Published December 30, 2023

Abstract: There is a demonstrated need for new chemotherapy options in pediatric oncology, as pediatric solid tumors continue to plateau at 60% with event-free survival. Imipridones, a novel class of small molecules, represent a potential new therapeutic option, with promising pre-clinical data and emerging clinical trial data in adult malignancies. ONC201, ONC206, and ONC212 are imipridones showing pro-apoptotic anti-cancer response. Using cell viability assays, and protein immunoblotting, we were able to demonstrate single-agent efficacy of all 3 imipridones inducing cell death in pediatric solid tumor cell lines, including osteosarcoma, malignant peripheral nerve sheath tumors, Ewing sarcoma (EWS), and neuroblastoma. ONC201 displayed IC50 values for non-H3K27M-mutated EWS cell lines ranging from 0.86 μM (SK-N-MC) to 2.76 μM (RD-ES), which were comparable to the range of IC50 values for H3K27M-mutated DIPG cells lines (range 1.06 to 1.56 μM). ONC212 demonstrated the highest potency in single-agent cell killing, followed by ONC206, and ONC201. Additionally, pediatric solid tumor cells were treated with single-agent therapy with histone deacetylase inhibitors (HDACi) vorinostat, entinostat, and panobinostat, showing cell killing with all 3 HDACi drugs, with panobinostat showing the greatest potency. We demonstrate that dual-agent therapy with combinations of imipridones and HDACi lead to synergistic cell killing and apoptosis in all pediatric solid tumor cell lines tested, with ONC212 and panobinostat combinations demonstrating maximal potency. The imipridones induced the integrated stress response with ATF4 and TRAIL receptor upregulation, as well as reduced expression of ClpX. Hyperacetylation of H3K27 was associated with synergistic killing of tumor cells following exposure to imipridone plus HDAC inhibitor therapies. Our results introduce a novel class of small molecules to treat pediatric solid tumors in a precision medicine framework. Use of impridones in pediatric oncology is novel and shows promising pre-clinical efficacy in pediatric solid tumors, including in combination with HDAC inhibitors.

Keywords: Pediatric solid tumor, imipridones, ONC201, ONC206, ONC212, pediatric cancer, histone deacetylase inhibitors, HDACi, Ewing sarcoma, osteosarcoma, neuroblastoma, malignant peripheral nerve sheath tumor, MPNST

Introduction

Pediatric chemotherapy treatment for sarcomas has remained stagnant for the past two decades [1, 2]. In the setting of relapse, progressive disease, or upfront metastasis, pediatric patients with sarcomas continue to have poor outcomes. After relapse or progression, which occurs in approximately 30-40% of patients, patients face a 5-year progression-free

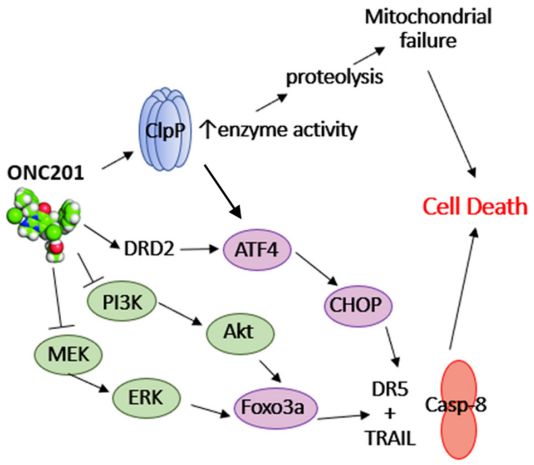

Figure 1. ONC201 and downstream effects leading to cell death.

survival of less than 10% [3-5]. Even more disappointingly, certain pediatric sarcomas, such as malignant peripheral nerve sheath tumors (MPNST), currently have no effective upfront chemotherapeutic options [6, 7]. Other pediatric solid tumors, such as neuroblastoma, has had a dramatic increase in survival, leading to current rates of around 60% event-free survival in metastatic, high-risk neuroblastoma, but with a plateau of efficacy in patients who are relapsed or refractory.

The need for new chemotherapy options is clear. Imipridones, a novel class of small molecules, represent a potential new therapeutic option in the management of pediatric solid tumor patients. Imipridones have been reported to antagonize the dopamine receptor D2 (DRD2) and D3 (DRD3), G protein-coupled receptors that are overexpressed in several malignancies. One such imipridone, ONC201/TIC10, is a novel agent that activates a potent innate immune pro-apoptotic anti-cancer response through the integrated stress response [8-10]. ONC201 (**Figure 1**) has been found to inactivate cell proliferation kinases Akt and ERK and to induce cell death through the pro-apoptotic tumor necrosis factor-related apoptosis-inducing ligand (TRAIL) [11-15]. Current pre-clinical and clinical trials have shown efficacy of ONC201 in adult or pediatric brain tumors with methionine mutations in histone H3 on lysine 27 (H3K27M-mutations) [16, 17]. ONC201 has potential for further development in pediatric solid tumors including in combination with epigenetic modulators [18].

It is becoming increasingly clear that the epigenetic landscape of pediatric solid tumors plays a role in tumorigenesis on a cellular basis. Fusion-positive pediatric sarcomas, such as Ewing sarcoma (EWS) and alveolar rhabdomyosarcoma, have aberrant activation of epigenetic pathways, including H3K27 [19-22]. Other pediatric sarcomas, such as MPNST, are found to have epigenetic modifications at H3K27, such as loss of trimethylation [23, 24]. This presents an opportunity for a novel precision medicine approach in pediatric sarcomas. In neuroblastoma, histone deacetylases (HDACs) play a role in in controlling MYCN function, which is amplified in more aggressive neuroblastoma; MYCN is also suspected to be an epigenetic modulator of histone hyperacetylation, leading to a more adrenergic cellular profile in high-risk chemotherapy-resistant neuroblastoma.

Mechanistically, cellular proliferation is inactivated by ONC201 through inhibition of Akt and ERK, and cell death is induced through the TRAIL pathway [8-10]. Prior *in vitro* studies of pediatric sarcomas, such as EWS, have produced promising results with ERK pathway inhibition, leading to apoptosis and inhibition of metastasis [25].

Thus, with all the complex interplay of epigenetics and cellular proliferation processes, we proposed to target pediatric solid tumors with a novel chemotherapeutic class, imipridones, and to investigate the synergy of an epigenetic modifying agent, HDAC inhibitors, in combination with imipridones. We proposed utilizing cell survival analyses, protein quantification, and flow cytometry to investigate markers of cell death. This is a unique approach of combining novel therapies for a patient population that continues to search for effective methods of combating difficult-to-treat disease.

Materials and methods

Cell culture and reagents

All cell lines were purchased from the American Type Culture Collection (ATCC). Cells were cultured in Eagle's Minimum Essential Medium supplemented with 10% fetal bovine serum (FBS), in RPMI-1640 medium supplemented 15% FBS, and in Dulbecco's Minimum Essential Medium supplemented with 10% fetal

Table 1. IC50 of tumor cell lines with ONC201 treatment (μM)

Cell Line	H3K27 mutation status	IC50 (μM)
SH-SY5Y *(MYCN non-amplified neuroblastoma)*	H3K27 with epigenetic changes leading to hyperacetylation	1.00
SU-DIPG-25 *(brain tumor)*	H3.3K27M (mutant) [26]	1.06
SU-DIPG-27 *(brain tumor)*	H3.3K27M (mutant) [26]	1.17
SU-DIPG-29 *(brain tumor)*	H3.3K27M (mutant) [26]	1.56
SK-N-MC *(EWS)*	H3K27 with epigenetic changes leading to hyperacetylation	0.86
sNF96.2 *(MPNST)*	H3K27me3 loss [27-29]	2.56
RD-ES *(EWS)*	H3K27 with epigenetic changes leading to hyperacetylation	2.76
U-2 OS *(osteosarcoma)*	H3K27me3 (wild-type, low expression) [30]	4.08
Saos-2 *(osteosarcoma)*	H3K27me3 (wild-type) [31]	5.71
SK-N-BE(2) *(MYCN amplified neuroblastoma)*	H3K27 with epigenetic changes leading to hyperacetylation	7.08

Half-maximal inhibitory concentration (IC50) of ONC201 when applied to pediatric solid tumor cell lines. With the addition of ONC201 IC50 results of our previously published work (Borsuk *et al.*) [27], there is a trend of increased sensitivity to ONC201 in cell lines with H3K27M mutations and in cell lines that have epigenetic changes leading to hyperacetylation at H3K27.

bovine serum (FBS). ONC201, ONC206, and ONC212 were obtained from Oncoceutics/Chimerix (Philadelphia, PA, USA). Panobinostat was purchased from MedKoo Biosciences Inc. (Morrisville, NC, USA). Entinostat and vorinostat were purchased from Selleck chemicals (Houston, TX, USA). All cell lines were incubated at 37°C in humidified atmosphere containing 5% CO_2.

Cell viability assay and synergy assessment

Cells were plated at a density of 3×10^3 cells per well of a 96-well plate. Cell viability was assessed using the CellTiter Glo assay (CTG, Promega, Madison, WI) and incubated at 37°C with 5% CO_2. Cells were subsequently treated with designated chemotherapeutic(s) at indicated concentrations. Cells were mixed with 25 μl of CellTiter-Glo reagents in 100 μl of culture volume, and bioluminescence imaging was measured using the Xenogen IVIS imager. Normalization of luminescence signals to control wells was used to determine percent of cell viability. Results are reported as % viability ± standard deviation. Dose response curves were generated, and the half maximal inhibitory concentration (IC50) was calculated using GraphPad Prism version 6 (San Diego, CA, USA). Compusyn software (ComboSyn, Inc.) was used to calculate combination indices (CI).

Western blots and antibodies

A total of 6×10^6 cells was seeded in media in a 6-well plate and incubated overnight at 37°C with 5% CO_2. Cells were subsequently treated with either vehicle or designated chemotherapeutic(s) at designated concentrations and returned to incubation.

After 72 hours, adherent cells were mechanically detached and washed with phosphate-buffered saline (PBS). Proteins were extracted from cells with RIPA buffer (Sigma-Aldrich, St. Louis, MO, USA). Protein concentration in extraction samples was determined using BCA protein Assay Kit (Thermo Fisher Scientific, Carlsbad, CA, USA). An equal amount of protein lysate was electrophoresed NuPAGE 4-12% Bis-Tris gel (Thermo Fisher Scientific) and transferred to polyvinylidene difluoride membrane (PVDF) membranes. The PVDF membrane was blocked with 5% non-fat milk (Sigma) in 1× PBS. Membranes were blocked with Tris-buffered saline with Tween 20 (TBST) with 5% w/v instant nonfat dry milk and incubated with primary antibody overnight at 4°C. Immunoblotting for proteins was performed using the following antibodies: Cell Signaling Technology Phospho-p44/42 MAPK (Erk1/2) (Thr202/Tyr204) (D13.14.4E) XP® Rabbit mAb #4370, Cell Signaling Technology p44/42 MAPK (Erk1/2) Antibody #9102, BD Biosciences Ran Antibody #610341, Cell Signaling Technology Caspase-8 Antibody #9746, Cell Signaling Technology cleaved PARP Antibody #9546, Santa Cruz Actin Antibody #sc8432, Cell Signaling Technology Acetyl Histone 3 #9649S, Cell Signaling Technology Phospho-PKA substrate Antibody #9521S, Cell Signaling Technology ATF4 Antibody #11815S, Abcam CLPX Antibody #Ab168338, Cell Signaling Technology Phospho-AKT Antibody #4060S, Santa Cruz CLPP Antibody #sc271284, and

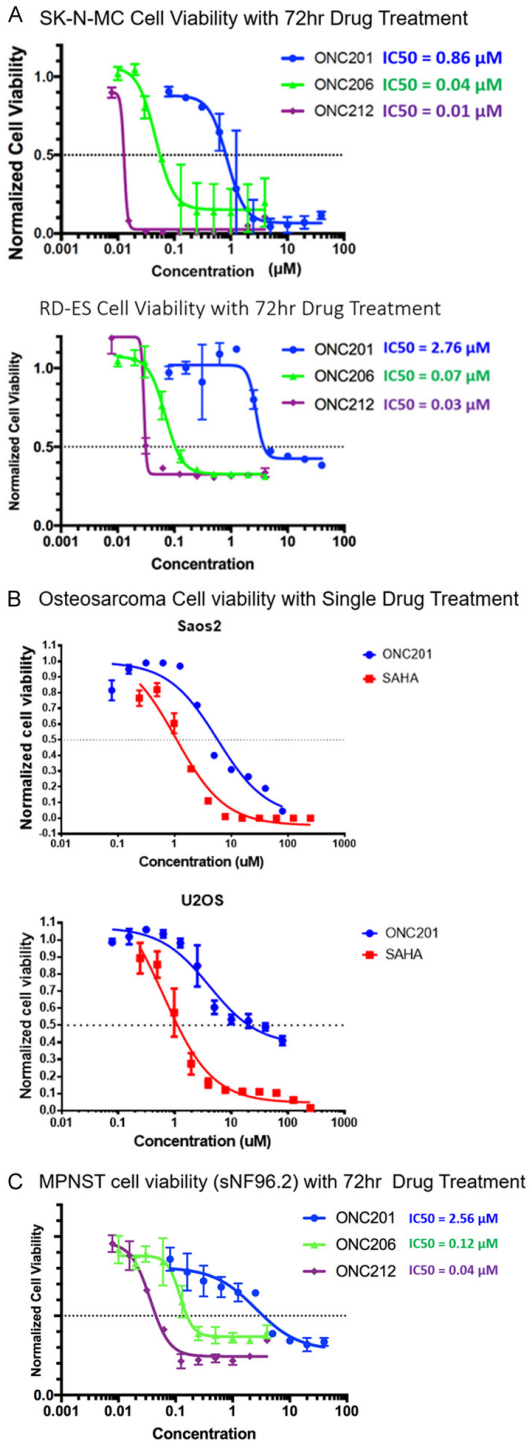

Figure 2. A. Pediatric solid tumor cell line IC50s after single drug treatment for a 72-hour incubation with imipridones (ONC201, ONC206, ONC212), assessed with CellTiter-Glo luminescent cell viability assay measuring ATP activity. B. Ewing sarcoma cell lines SK-N-MC and RD-ES drug treatment with imipridones. C. Osteosarcoma cell lines Saos2 and U2-OS with imipridone ONC201 drug treatment at 96 hours and 72 hours respectively.

BD Biosciences Cleaved Caspase 3 Antibody #559565.

Primary antibodies were diluted according to their datasheets. The primary antibodies indicated in the figures were incubated with the transferred PVDF in blocking buffer at 4°C overnight. Antibody binding was detected on PVDF with appropriate Pierce HRP-conjugated secondary antibodies by the Syngene imaging system. Invitrogen Goat anti-Rabbit IgG (H+L) Secondary Antibody, HRP #31460 and Goat anti-Mouse IgG (H+L) Secondary Antibody, HRP #31430 were diluted 1:5000 in 2.5% non-fat milk. Chemiluminescence reaction was detected using the ECL Reagent (Thermo Fisher Scientific). Ran and Vinculin were used as loading controls.

Statistics

Statistical analyses for cell viability assays were conducted using GraphPad Prism 6. Synergy analyses were conducted with Compusyn software and Synergy Finder software.

Results

Increased cell death with single agent drug treatment with imipridones

Drug treatments with imipridones on established pediatric cell lines were conducted. Osteosarcoma cell lines Saos-2 and U-2 OS, MPNST cell line sNF96.2, EWS cell lines SK-N-MC and RD-ES, MYCN amplified neuroblastoma cell line SK-N-BE(2), and non-MYCN amplified neuroblastoma cell line SK-SY5Y were treated with single-agent therapy, using ONC201 (**Table 1**), ONC206, and ONC212 (**Figure 2**). Tumor cell lines were most sensitive to ONC212 followed by ONC206 and ONC201.

Increased cell killing potency was noted with ONC206 compared to ONC201, and with ONC212 exhibiting the highest potency in all cell lines (**Figure 2**). In the neuroblastoma cell lines, imipridones demonstrated greater cell killing in the *MYCN* non-amplified cell line.

Increased cell death with single agent drug treatment with histone deacetylase inhibitors (HDACi)

Drug treatment with histone deacetylase inhibitors on established pediatric cell lines were

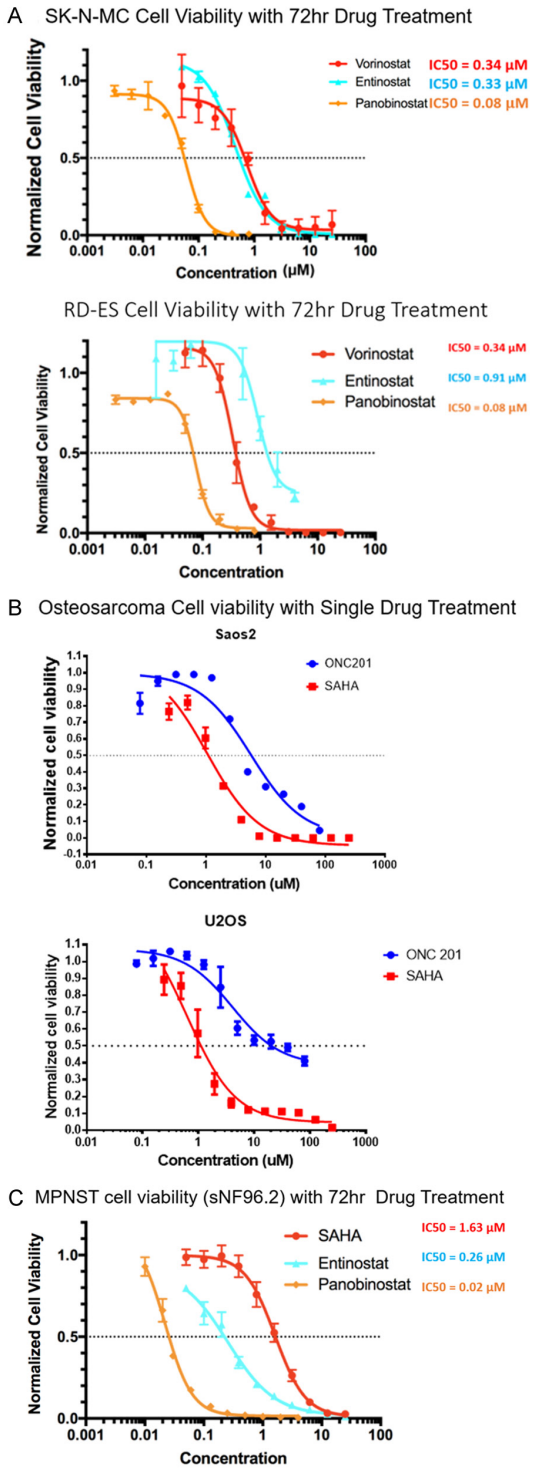

Figure 3. Pediatric solid tumor cell line IC50s after single drug treatment for a 72-hour incubation with HDACi (vorinostat, entinostat, panobinostat), assessed with CellTiter-Glo luminescent cell viability assay measuring ATP activity. A. Ewing sarcoma cell lines SK-N-MC and RD-ES drug treatment with HDACi. B. Osteosarcoma cell line Saos2 with HDACi drug treatment. C. Malignant peripheral nerve sheath tumor (MPNST) cell line sNF96.2 with HDACi drug treatment.

conducted. Osteosarcoma cell lines Saos-2 and U-2 OS, MPNST cell line sNF96.2, EWS cell lines SK-N-MC and RD-ES, MYCN amplified neuroblastoma cell line SK-N-BE(2), and non-MYCN amplified neuroblastoma cell line SK-SY5Y were treated with single-agent therapy, using vorinostat (SAHA), entinostat, and panobinostat.

In general, increased cell killing potency was noted with entinostat compared to vorinostat, and with panobinostat exhibiting the highest potency in all cell lines (**Figure 3**).

Increased cell death with combination treatment with imipridones and HDACi drugs

Cell viability studies and analysis with Compusyn demonstrate potent synergistic effects causing tumor cell death when imipridones are combined with HDAC inhibitors (**Figure 4**). Synergy calculations show that a wide range of doses of ONC201, ONC206, and ONC212, when combined with any of the 3 HDACi used in our experiments, have broadly synergistic effects in all the pediatric solid tumor cell lines tested.

Markers of cell death with combination treatment with imipridones and HDACi drugs

Using protein quantification studies and downstream target analysis on drug-treated cells, we investigated the mechanisms of how these therapies caused cell death. We showed that imipridones inactivate cell proliferation kinases Akt/ERK (**Figure 5**). Markers of cell death via protein analysis demonstrated that imipridones ONC201, ONC206, and ONC212 induced cell death, with increasing cleaved PARP levels as imipridone doses increased. Cleaved caspase 3 also increased with higher doses of imipridones, indicating that apoptotic mechanisms played a role in programmed cell death. Tumor cell apoptosis may occur by modifying the mitochondrial Clp protease complex, decreasing expression of chaperone subunit ClpX and activating mitochondrial proteolysis, seen most markedly with ONC201 drug treatment in all cell lines.

Our initial western blots in **Figure 5A** showed an increase in pERK levels in the SK-N-BE(2) and SH-SY5Y cell lines. The protein lysates were equally loaded despite significant cell death that was observed over 72 hours. We repeated

A SK-N-MC Cell Viability Showing Synergistic Cell Death with 72 Incubation with Combination Therapy

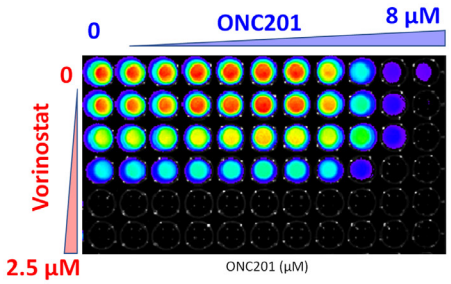

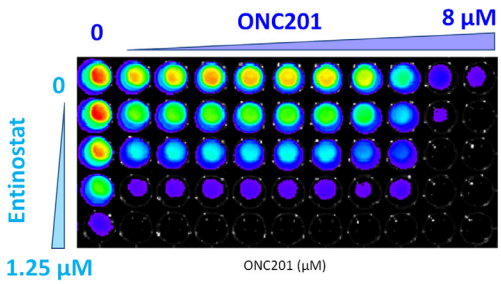

vorinostat (µM)

	0.016	0.031	0.063	0.125	0.25	0.50	1.00	2.00	4	8
0.16	0.75	0.81	1.24	1.36	3.14	2.82	2.36	0.98	0.45	0.36
0.31	1.07	1.03	1.11	1.21	1.54	1.69	2.09	1.98	0.68	0.35
0.63	1.23	1.18	1.23	1.22	1.31	1.37	1.37	0.87	0.46	0.38
1.25	0.85	0.85	0.84	0.82	0.88	0.88	0.85	0.68	0.53	0.44
2.50	1.06	1.06	1.06	1.017	1.02	1.02	0.97	0.97	0.92	0.86

entinostat (µM)

	0.016	0.031	0.063	0.125	0.25	0.5	1	2	4	8
0.16	0.33	0.34	0.38	0.45	0.61	0.86	1.03	0.74	0.22	0.13
0.31	0.42	0.43	0.44	0.45	0.49	0.57	0.57	0.60	0.20	0.14
0.63	0.50	0.51	0.52	0.52	0.52	0.54	0.51	0.60	0.33	0.25
1.25	0.64	0.65	0.65	0.65	0.66	0.67	0.66	0.72	0.54	0.43

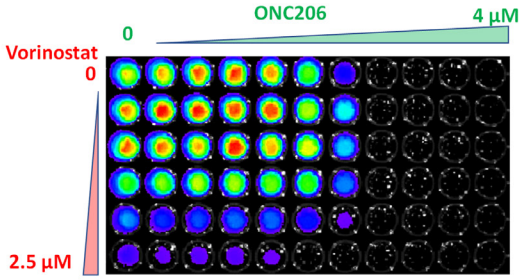

vorinostat (µM)

	0.016	0.031	0.063	0.125	0.25	0.5	1	2	4
0.16					4.79831	1.66735	0.75483	0.83436	1.54985
0.31						1.61587	0.84101	0.89915	1.45351
0.63	1.6817	2.60086	2.12539	1.96973	2.30595	1.59225	0.94411	0.93747	1.48509
1.25	0.71145	0.79237	0.92672	1.04506	1.09709	0.96709	0.63639	0.67777	1.41173
2.50	0.86683	0.93103	0.98866	0.95919	0.96787	0.70278	0.60241	0.77777	1.35555

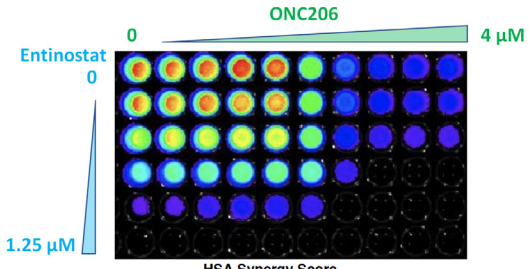

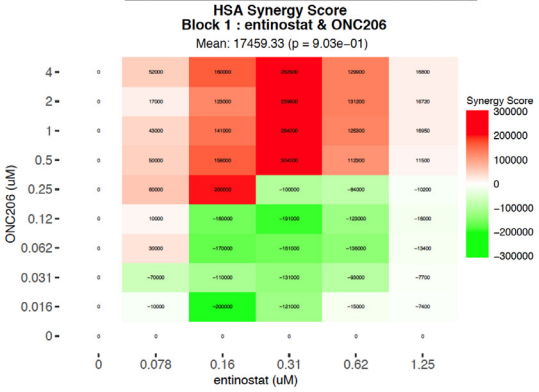

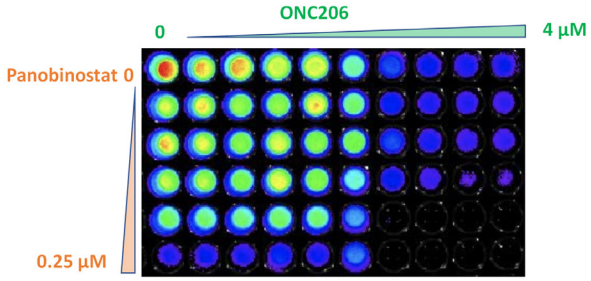

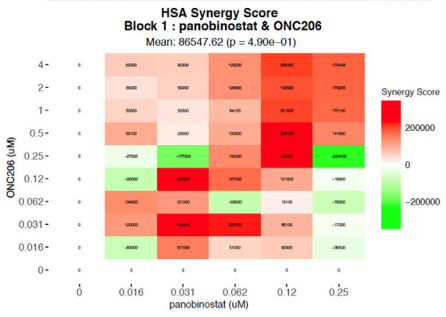

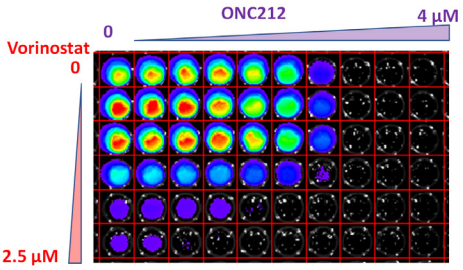

SKNMC vorinostat (μM)	ONC212 (μM) 0.016	0.031	0.063	0.125	0.25	0.5	1	2	4
0.16					2.17829	1.42144	0.68175	0.75406	1.1096
0.31					2.93589	1.6702	0.73884	0.68426	1.33383
0.63	1.13264	1.09064	1.19259	1.08027	1.12486	0.79045	0.60519	0.6054	1.36964
1.25	0.74369	0.71987	0.71793	0.61934	0.57012	0.4709	0.46467	0.66243	1.20987
2.50	1.18504	0.99782	1.01498	0.73481	0.60579	0.55975	0.5037	0.77742	1.32487

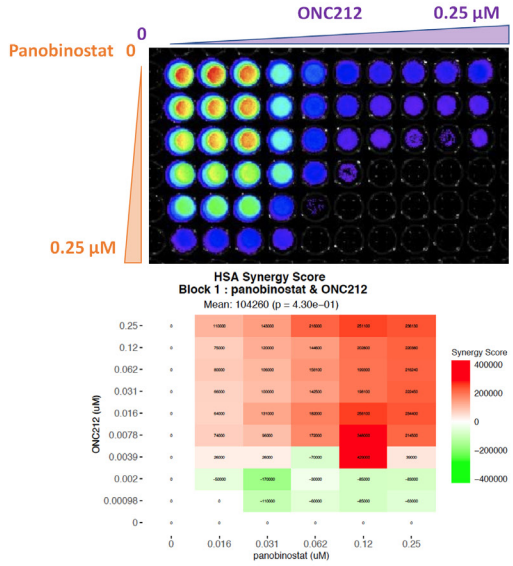

B

RD-ES (EWS) Cell Viability Showing Synergy with Combination Therapy

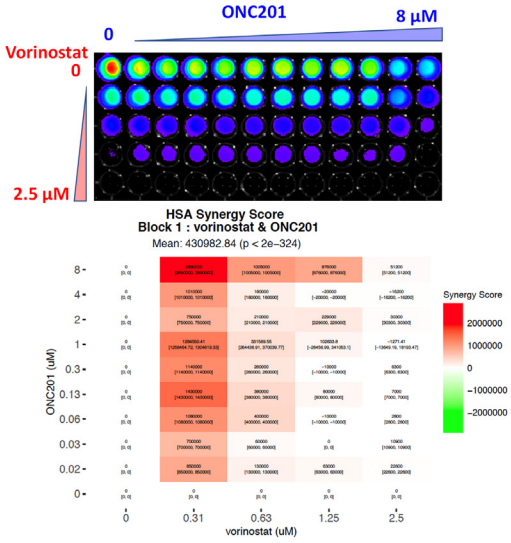

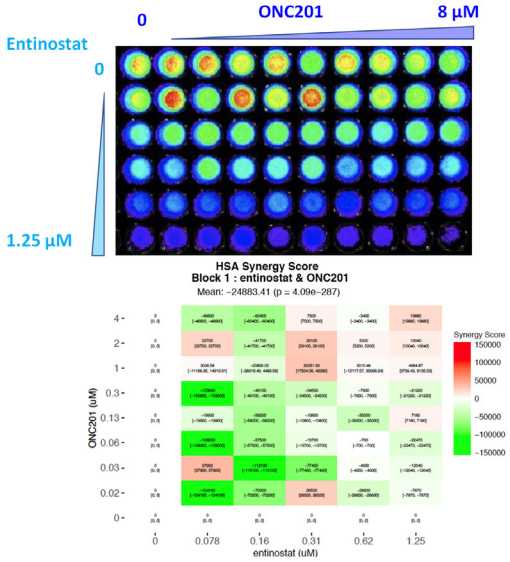

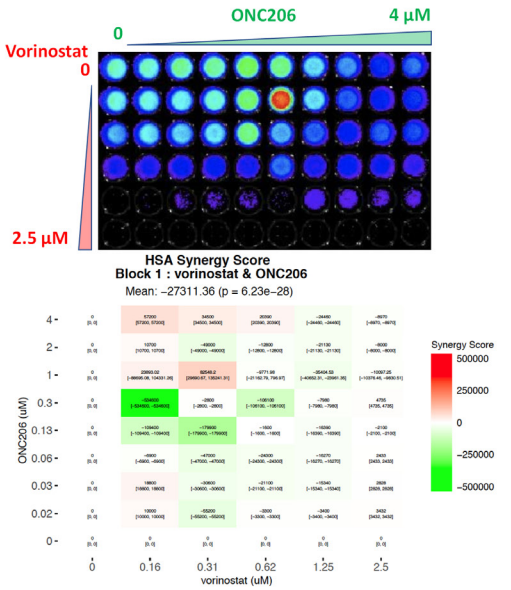

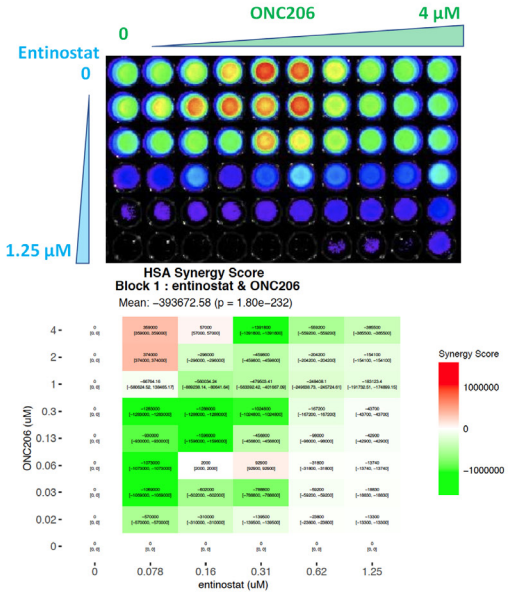

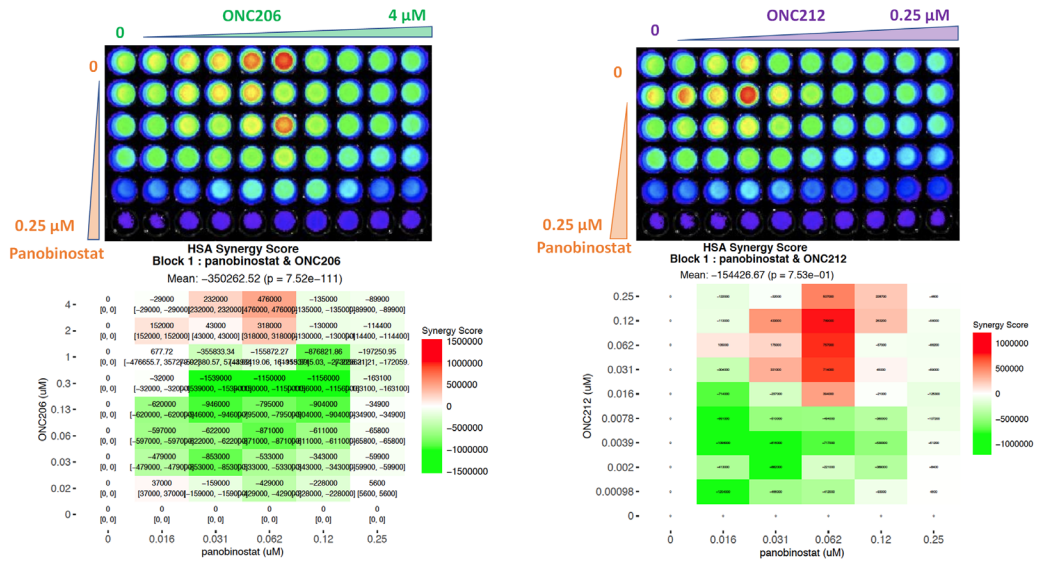

C

Osteosarcoma cell viability showing synergy with combination therapy

U2-OS

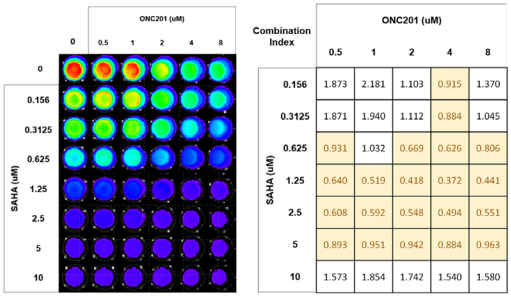

Combination Index	ONC201 (uM) 0.5	1	2	4	8
SAHA (uM) 0.156	1.873	2.181	1.103	0.915	1.370
0.3125	1.871	1.940	1.112	0.884	1.045
0.625	0.931	1.032	0.669	0.626	0.806
1.25	0.640	0.519	0.418	0.372	0.441
2.5	0.608	0.592	0.548	0.494	0.551
5	0.893	0.951	0.942	0.884	0.963
10	1.573	1.854	1.742	1.540	1.580

Saos-2

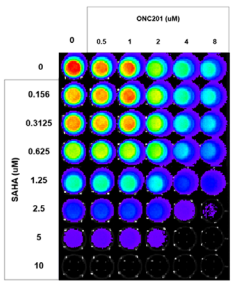

Combination Index	ONC201 (uM) 0.5	1	2	4	8
SAHA (uM) 0.156	1.17	2.86	1.49	0.83	1.21
0.3125	1.65	2.74	1.76	0.94	1.13
0.625	1.73	2.02	2.17	0.96	1.10
1.25	1.51	1.60	1.44	0.83	0.81
2.5	1.38	1.42	1.39	0.51	0.30
5	0.97	1.00	0.75	0.24	0.27
10	0.64	0.66	0.51	0.48	0.50

D

MPNST (sNF96.2) cell viability showing synergy with combination therapy

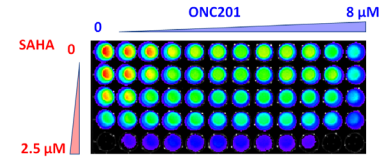

sNF96.2 SAHA (μM)	ONC201 (μM) 0.016	0.031	0.063	0.125	0.25	0.50	1.00	2.00	4.00	8
0.31	0.70757	0.36552	0.35582	0.43706	0.46895	0.59024	2.13795	3.72481	10.2232	0.71505
0.63	0.62273	0.60114	0.60571	0.52659	0.53892	0.63266	0.77739	0.9768	1.32278	0.553
1.25	1.1028	1.1105	1.08559	0.97637	0.9839	1.05247	1.04656	1.08967	1.12352	0.75098
2.50	1.0434	1.123	1.10696	1.14695	1.07163	0.99435	1.01821	0.88384	0.5889	0.41668

E

Neuroblastoma Cell Viability Showing Synergy with Combination Therapy

SK-N-BE(2)

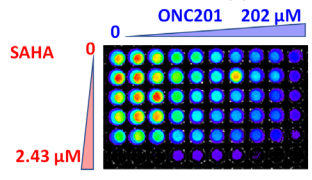

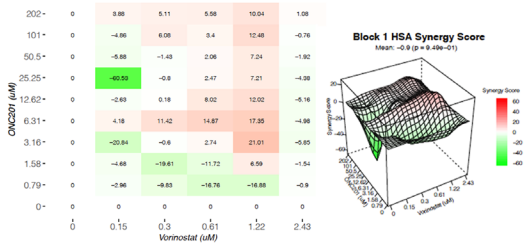

SK-N-BE(2)

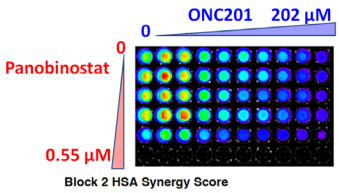

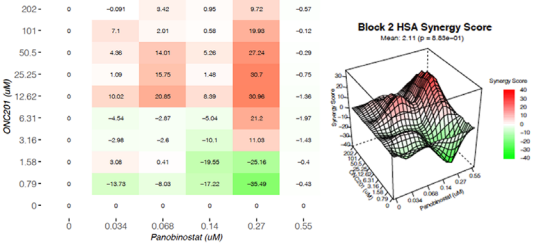

Figure 4. *In vitro* studies of pediatric solid tumor cell lines treated with 72-hour incubation of increasing dose combinations of imipridones with HDAC inhibitors. Cell viability assessed using CellTiter-Glo. Combination index obtained with CompuSyn software (ComboSyn, Inc.) shown in yellow and white boxes below. A. Synergistic dose combination indices of <1.0 are in yellow. B. Cell viability and synergy of Ewing sarcoma cell line SK-N-MC after 72-hour drug combination treatment with HDACi and imipridones. C. Cell viability and synergy of Ewing sarcoma cell line RD-ES after 72-hour drug combination treatment with HDACi and imipridones. D. Cell viability and synergy of osteosarcoma cell lines U2-OS and Saos-2 after 72-hour drug combination treatment and 96-hour drug combination treatment with vorinostat (SAHA) and ONC201, respectively. E. Cell viability and synergy of MPNST cell line sNF96.2 after 72-hour drug combination treatment with HDACi and imipridones. Cell viability and synergy of neuroblastoma cell lines SK-N-BE(2) and SK-SY5Y after 72-hour drug combination treatment with HDACi and imipridones.

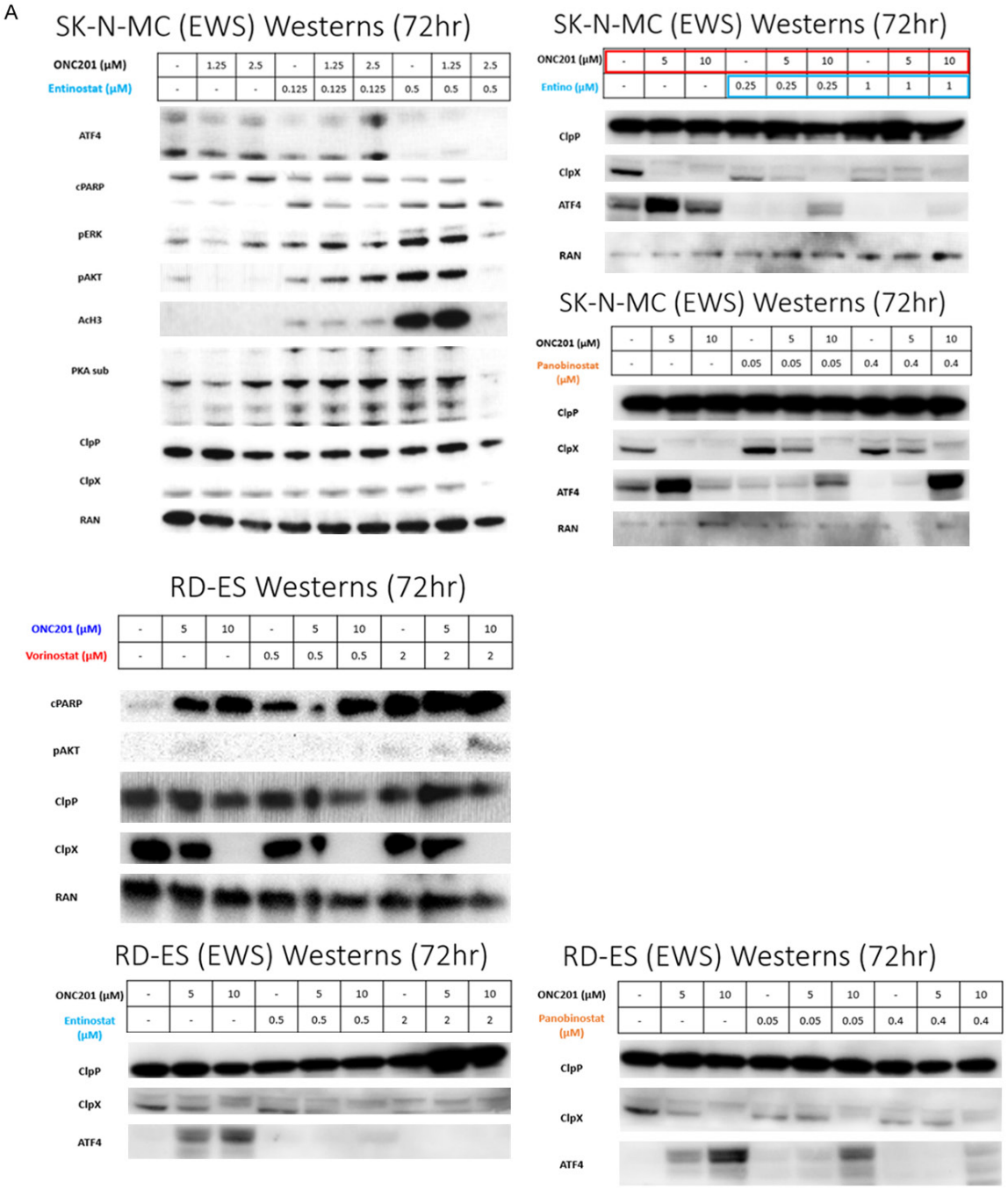

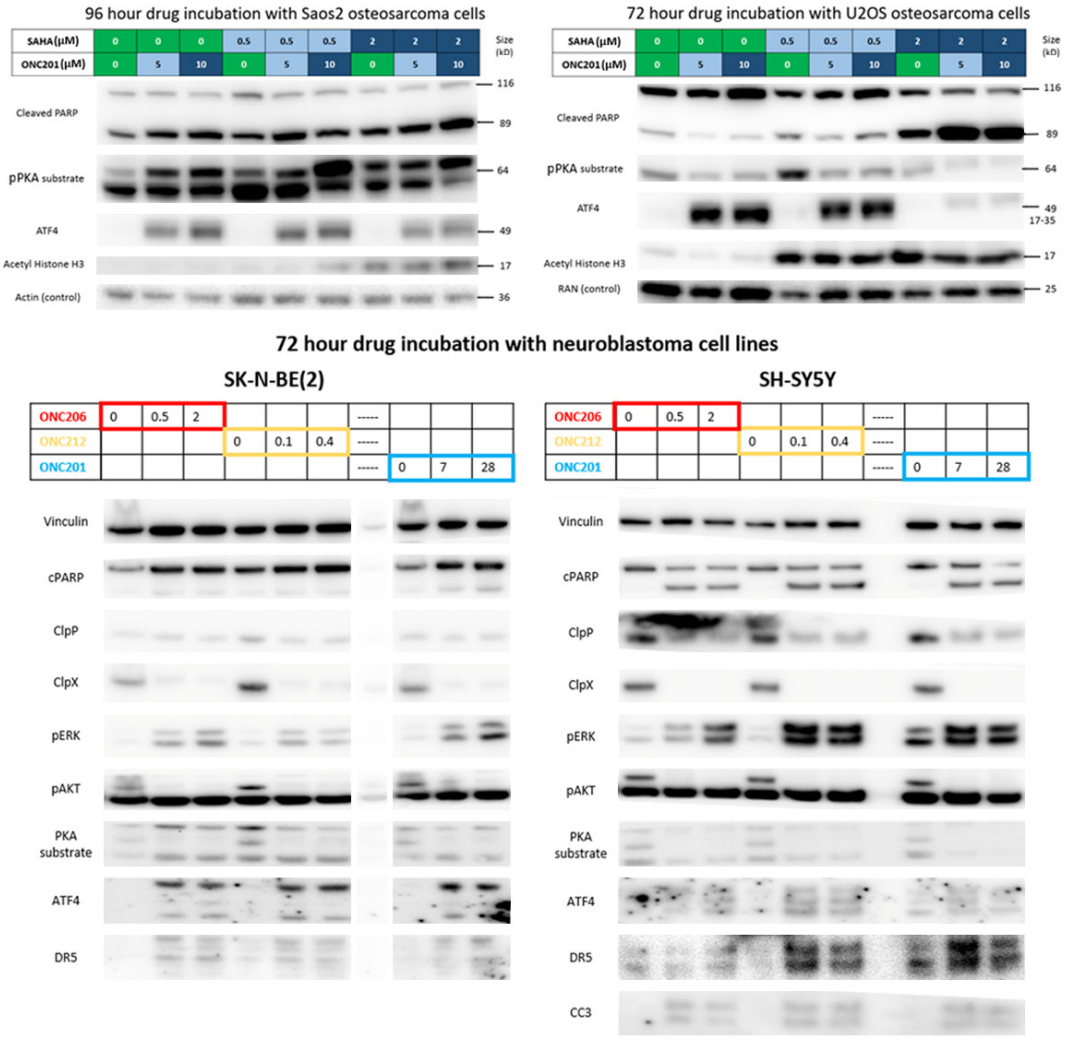
96 hour drug incubation with Saos2 osteosarcoma cells
SAHA (μM)
ONC201 (μM)
Size (kD)
Cleaved PARP
pPKA substrate
ATF4
Acetyl Histone H3
Actin (control)
72 hour drug incubation with U2OS osteosarcoma cells
RAN (control)
72 hour drug incubation with neuroblastoma cell lines
SK-N-BE(2)
SH-SY5Y
ONC206
ONC212
ONC201
Vinculin
cPARP
ClpP
ClpX
pERK
pAKT
PKA substrate
DR5
CC3

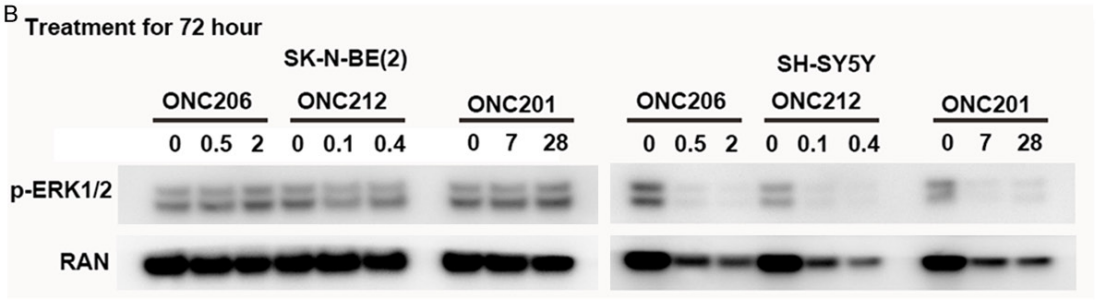
B
Treatment for 72 hour
SK-N-BE(2)
SH-SY5Y
ONC206
ONC212
ONC201
0 0.5 2
0 0.1 0.4
0 7 28
p-ERK1/2
RAN

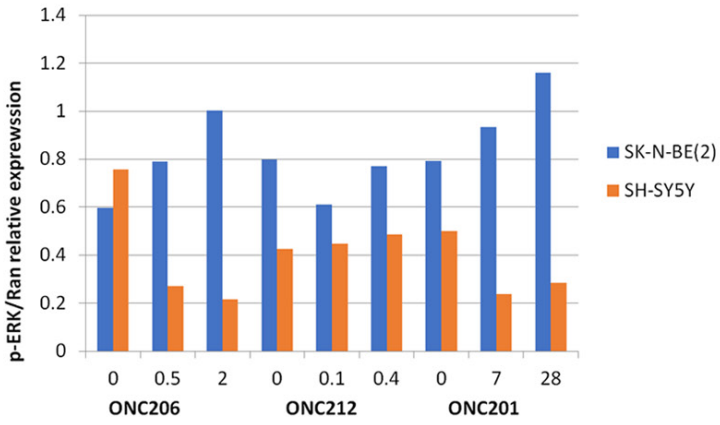
p-ERK/Ran relative exprewssion
1.4
1.2
1
0.8
0.6
0.4
0.2
0
0 0.5 2 0 0.1 0.4 0 7 28
ONC206
ONC212
ONC201
SK-N-BE(2)
SH-SY5Y

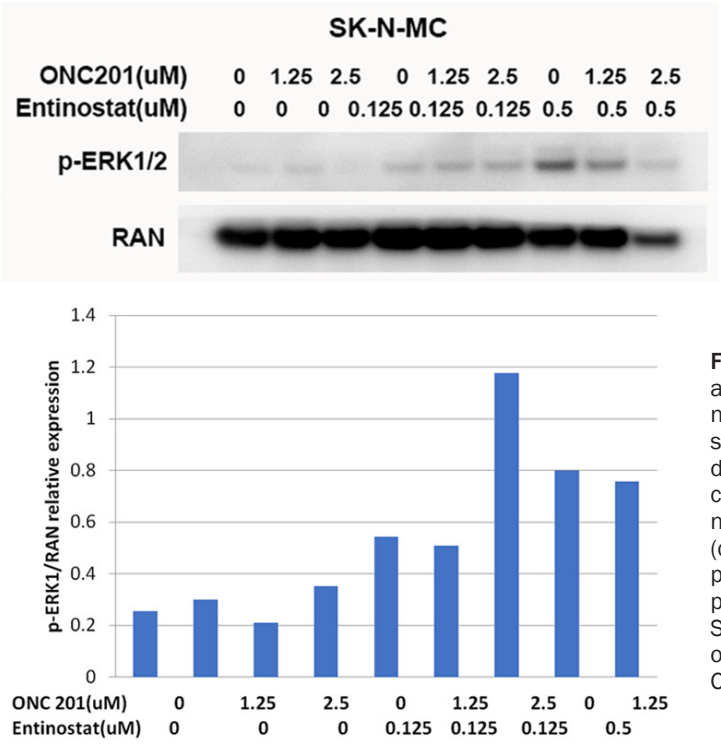

Figure 5. Protein immunoblotting analysis showing 72-hour combination drug treatment of pediatric solid tumor cells in vitro with imipridones and HDACi. A. Increasing concentrations of drugs in combination leads to increased cell death (cleaved PARP) and suppression of pAKT and pERK. B. Alterations in pERK in SK-N-MC, SK-N-BE(2) and SH-SY5Y cell lines treated with various doses of imipridones ONC201, ONC206, or ONC212.

the experiments with imipridones ONC201, ONC206, and ONC212 in the SK-N-BE(2) and SH-SY5Y cell lines (**Figure 5B**). Neither cell line had much increase in pERK. Both experiments showed decreased viability at 72 hours. In the first experiment where loading was equal, there was likely enrichment for viable cells while in the second experiment there was more clear reduction in pERK. For SH-SY5Y cells, the repeat experiment showed a decrease in pERK with ONC206, ONC212, and ONC201 at several doses. In SK-N-MC cells, pERK decreased with the ONC201 plus entinostat combination.

Discussion

Our work demonstrates that imipridones are a potent novel therapy that shows great promise in the treatment of pediatric solid tumors. We show that imipridones inactivate cellular proliferation in pediatric sarcomas through the Akt/ERK pathway. Protein quantification by Western blotting revealed treatment with imipridone ONC201 affected the mitochondrial Clp protease complex by decreasing the chaperone subunit ClpX. Cell viability studies and analysis with Compusyn demonstrate potent synergistic effects causing tumor cell death when imipridones are combined with HDAC inhibitors.

Preclinical studies with the imipridone ONC201 in H3K27-mutated brain tumors have shown promising results, and Phase I/II clinical trials investigating the effects of ONC201 in patients with H3K27-mutated adult tumors are currently underway. Mechanistically, cellular proliferation is inactivated by ONC201 through the Akt/ERK pathway, and cell death is induced through the TRAIL pathway. We show ERK pathway inhibition, leading to apoptosis and inhibition of metastasis. We also demonstrate changes in the mitochondrial pathway, with decreases in mitochondrial machinery ClpX seen with increasing doses of ONC201.

Pediatric sarcomas with chromosomal translocations are driven by the disease-causing fusion protein with downstream cell-proliferation pathway effects, including H3K27 [32]. Tumor cell lines harboring H3K27 mutations display remarkable sensitivity to ONC201 and other imipridones. We noted that cell death with single-agent imipridone treatments were higher in mutant H3K27 cell lines compared to wild-type H3K27 cell lines. Our work brings up the question if epigenetic changes in pediatric solid tumors lead to increased sensitivity to imipridones due to downstream H3K27 epigenetic modifications (**Figure 6**). H3K27-modifi-

A

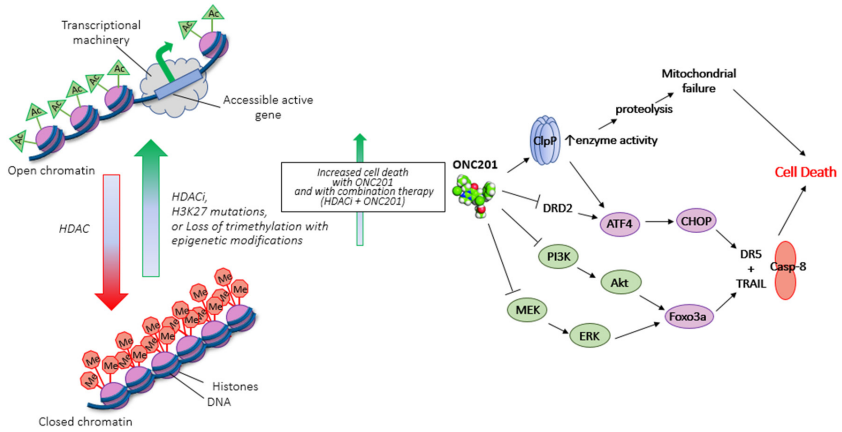
Novel therapeutic combination of Imipridones and HDAC inhibitors leading to cell death
Transcriptional machinery
Accessible active gene
Open chromatin
HDAC
HDACi, H3K27 mutations, or Loss of trimethylation with epigenetic modifications
Closed chromatin
Histones
DNA
Increased cell death with ONC201 and with combination therapy (HDACi + ONC201)
ONC201
ClpP
↑enzyme activity
proteolysis
Mitochondrial failure
Cell Death
DRD2
ATF4
CHOP
PI3K
Akt
MEK
ERK
Foxo3a
DR5 + TRAIL
Casp-8

B

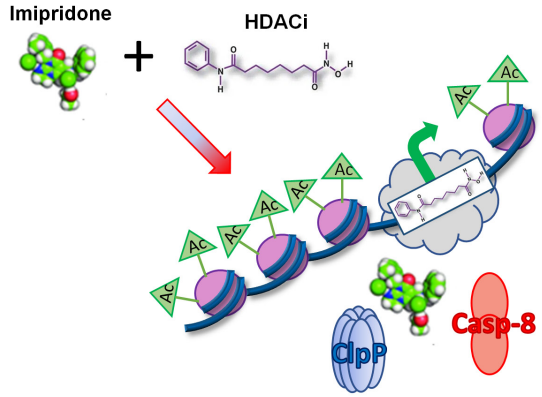
Imipridone
HDACi
Ac
ClpP
Casp-8

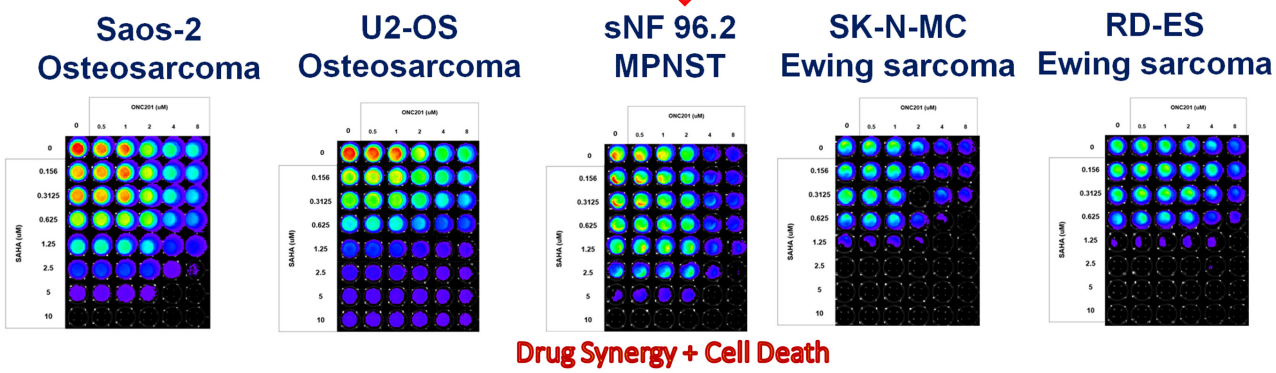
Saos-2 Osteosarcoma
U2-OS Osteosarcoma
sNF 96.2 MPNST
SK-N-MC Ewing sarcoma
RD-ES Ewing sarcoma
Drug Synergy + Cell Death

Figure 6. Hypothesized mechanism of action of Imipridones and HDACi drug synergy leading to increased cell death with combination therapy.

cations, such as loss of trimethylation or increased acetylation due to oncogenic fusion drivers, may confer increased anti-tumor effects of imipridones.

Our results introduce a novel class of small molecules to treat pediatric solid tumors in a precision medicine framework. Use of imipridones in pediatric oncology is novel and shows pre-clinical efficacy in inducing cell death. Synergy studies with HDACi and imipridones consistently demonstrate increased cell killing via a pro-apoptotic anti-cancer effect through the integrated stress response. Results from our work provides the pre-clinical background for this new class of drugs to be developed into Phase I/II clinical studies as a first-in-class therapy for pediatric solid tumors. Future directions include opening Phase I/II clinical trials for pediatric sarcomas once pre-clinical data is obtained from this study. Preclinical strategies to target gene fusions include both the utilization of existing inhibitors as well as the development of novel drugs through rational design approaches. The development of novel therapies requires a significant development time and multidisciplinary effort that includes expertise in genomics, molecular biology, pharmacology, clinical trials, and clinical oncology. Using these resources more effectively will not only help drive the development of novel therapies, but also better inform individual patient treatment decisions. As our understanding of the molecular drivers of pediatric fusion-positive cancers increases, so do our abilities to tailor therapies toward better outcomes for this patient population.

Acknowledgements

W.S.E-D. is an American Cancer Society Research Professor and is supported by the Mencoff Family University Professorship at Brown University. The authors thank Dr. Michelle Monje at Stanford University for DIPG cell lines. This work was supported by a grant from the Rhode Island Foundation (W-I.C.) and an NIH grant (CA173453) to W.S.E-D.

Disclosure of conflict of interest

W-I.C. is an employee of AstraZeneca. The work described in this publication was conducted in its entirety at Brown University, and it predates Dr. Chang's employment at AstraZeneca.

Address correspondence to: Wen-I Chang and Wafik S El-Deiry, Laboratory of Translational Oncology and Translational Cancer Therapeutics, Warren Alpert Medical School of Brown University, Providence, RI, USA. E-mail: wen.i.chang.md@gmail.com (WIC); wafik@brown.edu (WSED)

References

[1] Yohe ME, Heske CM, Stewart E, Adamson PC, Ahmed N, Antonescu CR, Chen E, Collins N, Ehrlich A, Galindo RL, Gryder BE, Hahn H, Hammond S, Hatley ME, Hawkins DS, Hayes MN, Hayes-Jordan A, Helman LJ, Hettmer S, Ignatius MS, Keller C, Khan J, Kirsch DG, Linardic CM, Lupo PJ, Rota R, Shern JF, Shipley J, Sindiri S, Tapscott SJ, Vakoc CR, Wexler LH and Langenau DM. Insights into pediatric rhabdomyosarcoma research: challenges and goals. Pediatr Blood Cancer 2019; 66: e27869.

[2] Pappo AS and Dirksen U. Rhabdomyosarcoma, Ewing sarcoma, and other round cell sarcomas. J Clin Oncol 2018; 36: 168-179.

[3] Stahl M, Ranft A, Paulussen M, Bölling T, Vieth V, Bielack S, Görtitz I, Braun-Munzinger G, Hardes J, Jürgens H and Dirksen U. Risk of recurrence and survival after relapse in patients with Ewing sarcoma. Pediatr Blood Cancer 2011; 57: 549-53.

[4] Duchman KR, Gao Y and Miller BJ. Prognostic factors for survival in patients with Ewing's sarcoma using the surveillance, epidemiology, and end results (SEER) program database. Cancer Epidemiol 2015; 39: 189-95.

[5] Smeland S, Bielack SS, Whelan J, Bernstein M, Hogendoorn P, Krailo MD, Gorlick R, Janeway KA, Ingleby FC, Anninga J, Antal I, Arndt C, Brown KLB, Butterfass-Bahloul T, Calaminus G, Capra M, Dhooge C, Eriksson M, Flanagan AM, Friedel G, Gebhardt MC, Gelderblom H, Goldsby R, Grier HE, Grimer R, Hawkins DS, Hecker-Nolting S, Sundby Hall K, Isakoff MS, Jovic G, Kühne T, Kager L, von Kalle T, Kabickova E, Lang S, Lau CC, Leavey PJ, Lessnick SL, Mascarenhas L, Mayer-Steinacker R, Meyers PA, Nagarajan R, Randall RL, Reichardt P, Renard M, Rechnitzer C, Schwartz CL, Strauss S, Teot L, Timmermann B, Sydes MR and Marina N. Survival and prognosis with osteosarcoma: outcomes in more than 2000 patients in the EURAMOS-1 (European and American Osteosarcoma Study) cohort. Eur J Cancer 2019; 109: 36-50.

[6] Higham CS, Steinberg SM, Dombi E, Perry A, Helman LJ, Schuetze SM, Ludwig JA, Staddon A, Milhem MM, Rushing D, Jones RL, Livingston M, Goldman S, Moertel C, Wagner L, Janhofer D, Annunziata CM, Reinke D, Long L, Viskochil D, Baker L and Widemann BC. SARC006: phase II trial of chemotherapy in sporadic and neurofibromatosis type 1 associated chemotherapy-naive malignant peripheral nerve sheath tumors. Sarcoma 2017; 2017: 8685638.

[7] Widemann BC, Lu Y, Reinke D, Okuno SH, Meyer CF, Cote GM, Chugh R, Milhem MM, Hirbe AC, Kim A, Turpin B, Pressey JG, Dombi E, Jayaprakash N, Helman LJ, Onwudiwe N, Cichowski K and Perentesis JP. Targeting sporadic and neurofibromatosis type 1 (NF1) related refractory malignant peripheral nerve sheath tumors (MPNST) in a phase II study of everolimus in combination with bevacizumab (SARC016). Sarcoma 2019; 2019: 7656747.

[8] Kline CL, van den Heuvel AP, Allen JE, Prabhu VV, Dicker DT and El-Deiry WS. ONC201 kills solid tumor cells by triggering an integrated stress response dependent on ATF4 activation by specific eIF2α kinases. Sci Signal 2016; 9: ra18.

[9] Allen JE, Krigsfeld G, Mayes PA, Patel L, Dicker DT, Patel AS, Dolloff NG, Messaris E, Scata KA, Wang W, Zhou JY, Wu GS and El-Deiry WS. Dual inactivation of Akt and ERK by TIC10 signals Foxo3a nuclear translocation, TRAIL gene induction, and potent antitumor effects. Sci Transl Med 2013; 5: 171ra17.

[10] Prabhu VV, Morrow S, Rahman Kawakibi A, Zhou L, Ralff M, Ray J, Jhaveri A, Ferrarini I, Lee Y, Parker C, Zhang Y, Borsuk R, Chang WI, Honeyman JN, Tavora F, Carneiro B, Raufi A, Huntington K, Carlsen L, Louie A, Safran H, Seyhan AA, Tarapore RS, Schalop L, Stogniew M, Allen JE, Oster W and El-Deiry WS. ONC201 and imipridones: anti-cancer compounds with clinical efficacy. Neoplasia 2020; 22: 725-744.

[11] Ray JE, Ralff MD, Jhaveri A, Zhou L, Dicker DT, Ross EA and El-Deiry WS. Antitumorigenic effect of combination treatment with ONC201 and TRAIL in endometrial cancer *in vitro* and *in vivo*. Cancer Biol Ther 2021; 22: 554-563.

[12] Ralff MD, Kline CLB, Küçükkase OC, Wagner J, Lim B, Dicker DT, Prabhu VV, Oster W and El-Deiry WS. ONC201 demonstrates antitumor effects in both triple-negative and non-triple-negative breast cancers through TRAIL-dependent and TRAIL-independent mechanisms. Mol Cancer Ther 2017; 16: 1290-1298.

[13] Prabhu VV, Talekar MK, Lulla AR, Kline CLB, Zhou L, Hall J, Van den Heuvel APJ, Dicker DT, Babar J, Grupp SA, Garnett MJ, McDermott U, Benes CH, Pu JJ, Claxton DF, Khan N, Oster W, Allen JE and El-Deiry WS. Single agent and synergistic combinatorial efficacy of first-in-class small molecule imipridone ONC201 in hematological malignancies. Cell Cycle 2018; 17: 468-478.

[14] Allen JE, Kline CL, Prabhu VV, Wagner J, Ishizawa J, Madhukar N, Lev A, Baumeister M, Zhou L, Lulla A, Stogniew M, Schalop L, Benes C, Kaufman HL, Pottorf RS, Nallaganchu BR, Olson GL, Al-Mulla F, Duvic M, Wu GS, Dicker DT, Talekar MK, Lim B, Elemento O, Oster W, Bertino J, Flaherty K, Wang ML, Borthakur G, Andreeff M, Stein M and El-Deiry WS. Discovery and clinical introduction of first-in-class imipridone ONC201. Oncotarget 2016; 7: 74380-74392.

[15] Allen JE, Krigsfeld G, Patel L, Mayes PA, Dicker DT, Wu GS and El-Deiry WS. Identification of TRAIL-inducing compounds highlights small molecule ONC201/TIC10 as a unique anti-cancer agent that activates the TRAIL pathway. Mol Cancer 2015; 14: 99.

[16] Arrillaga-Romany I, Chi AS, Allen JE, Oster W, Wen PY and Batchelor TT. A phase 2 study of the first imipridone ONC201, a selective DRD2 antagonist for oncology, administered every three weeks in recurrent glioblastoma. Oncotarget 2017; 8: 79298-79304.

[17] Chi AS, Tarapore RS, Hall MD, Shonka N, Gardner S, Umemura Y, Sumrall A, Khatib Z, Mueller S, Kline C, Zaky W, Khatua S, Weathers SP, Odia Y, Niazi TN, Daghistani D, Cherrick I, Korones D, Karajannis MA, Kong XT, Minturn J, Waanders A, Arillaga-Romany I, Batchelor T, Wen PY, Merdinger K, Schalop L, Stogniew M, Allen JE, Oster W and Mehta MP. Pediatric and adult H3 K27M-mutant diffuse midline glioma treated with the selective DRD2 antagonist ONC201. J Neurooncol 2019; 145: 97-105.

[18] Zhang Y, Zhou L, Borsuk R, Lulla R, Tapinos N, Safran H, Seyhan AA and El-Deiry WS. EZH2i EPZ-6438 and HDACi vorinostat synergize with ONC201/TIC10 to activate integrated stress response, DR5, reduce H3K27 methylation, ClpX and promote apoptosis of multiple tumor types including DIPG. Neoplasia 2021; 23: 792-810.

[19] Gryder BE, Yohe ME, Chou HC, Zhang X, Marques J, Wachtel M, Schaefer B, Sen N, Song Y, Gualtieri A, Pomella S, Rota R, Cleveland A, Wen X, Sindiri S, Wei JS, Barr FG, Das S, Andresson T, Guha R, Lal-Nag M, Ferrer M, Shern JF, Zhao K, Thomas CJ and Khan J. PAX3-FOXO1 establishes myogenic super enhancers and confers BET bromodomain vulnerability. Cancer Discov 2017; 7: 884-899.

[20] Tomazou EM, Sheffield NC, Schmidl C, Schuster M, Schönegger A, Datlinger P, Kubicek S, Bock C and Kovar H. Epigenome mapping reveals distinct modes of gene regulation and

widespread enhancer reprogramming by the oncogenic fusion protein EWS-FLI1. Cell Rep 2015; 10: 1082-95.
[21] Charville GW, Wang WL, Ingram DR, Roy A, Thomas D, Patel RM, Hornick JL, van de Rijn M and Lazar AJ. EWSR1 fusion proteins mediate PAX7 expression in Ewing sarcoma. Mod Pathol 2017; 30: 1312-1320.
[22] Shen JK, Cote GM, Gao Y, Choy E, Mankin HJ, Hornicek FJ and Duan Z. Targeting EZH2-mediated methylation of H3K27 inhibits proliferation and migration of synovial sarcoma in vitro. Sci Rep 2016; 6: 25239.
[23] Otsuka H, Kohashi K, Yoshimoto M, Ishihara S, Toda Y, Yamada Y, Yamamoto H, Nakashima Y and Oda Y. Immunohistochemical evaluation of H3K27 trimethylation in malignant peripheral nerve sheath tumors. Pathol Res Pract 2018; 214: 417-425.
[24] Schaefer IM, Fletcher CD and Hornick JL. Loss of H3K27 trimethylation distinguishes malignant peripheral nerve sheath tumors from histologic mimics. Mod Pathol 2016; 29: 4-13.
[25] Chandhanayingyong C, Kim Y, Staples JR, Hahn C and Lee FY. MAPK/ERK signaling in osteosarcomas, Ewing sarcomas and chondrosarcomas: therapeutic implications and future directions. Sarcoma 2012; 2012: 404810.
[26] Borsuk R, Zhou L, Chang WI, Zhang Y, Sharma A, Prabhu VV, Tapinos N, Lulla RR and El-Deiry WS. Potent preclinical sensitivity to imipridone-based combination therapies in oncohistone H3K27M-mutant diffuse intrinsic pontine glioma is associated with induction of the integrated stress response, TRAIL death receptor DR5, reduced CLpX and apoptosis. Am J Cancer Res 2021; 11: 4607-4623.
[27] Pemov A, Li H, Presley W, Wallace MR and Miller DT. Genetics of human malignant peripheral nerve sheath tumors. Neurooncol Adv 2019; 2 Suppl 1: i50-i61.
[28] Zhang X, Murray B, Mo G and Shern JF. The role of polycomb repressive complex in malignant peripheral nerve sheath tumor. Genes (Basel) 2020; 11: 287.
[29] Korfhage J and Lombard DB. Malignant peripheral nerve sheath tumors: from epigenome to bedside. Mol Cancer Res 2019; 17: 1417-1428.
[30] Feng H, Tillman H, Wu G, Davidoff AM and Yang J. Frequent epigenetic alterations in polycomb repressive complex 2 in osteosarcoma cell lines. Oncotarget 2018; 9: 27087-27091.
[31] Piunti A, Smith ER, Morgan MAJ, Ugarenko M, Khaltyan N, Helmin KA, Ryan CA, Murray DC, Rickels RA, Yilmaz BD, Rendleman EJ, Savas JN, Singer BD, Bulun SE and Shilatifard A. CATACOMB: an endogenous inducible gene that antagonizes H3K27 methylation activity of Polycomb repressive complex 2 via an H3K27M-like mechanism. Sci Adv 2019; 5: eaax2887.
[32] Feng FY, Brenner JC, Hussain M and Chinnaiyan AM. Molecular pathways: targeting ETS gene fusions in cancer. Clin Cancer Res 2014; 20: 4442-8.